# Photo-driven effects in nano-soft composites with liquid crystal/polymer hosts

Final synopsis of the thesis

in Physics

*Submitted by*

Pragnya Satapathy
Senior Research Fellow
Registration No- Ref: No.MU/EXB/Ph.D./CR.17/Phy./2020-21/E.13
Enrollment number-178105118
Centre for Nano and Soft Matter Sciences
Bengaluru-562162

*Under the Supervision of*

Dr. S. Krishna Prasad

Centre for Nano and Soft Matter Sciences (CeNS),
Shivanapura, Bangalore- 562162

## Introduction

Liquid crystals (LCs) are states of matter which simultaneously have properties of a liquid, such as fluidity, and of crystals with characteristics such as anisotropy in dielectric and optical properties [1-5]. For example, the presence of anisotropy in the optical properties gives different refractive index values measured along and perpendicular to the director, making the materials birefringent. Depending upon the shape anisotropy, thermotropic LC molecules are generally elongated rod-like (calamitic) or disk-like (discotic); in recent times, banana-shaped molecules showing LC phase have attracted much attention. Nematic (N) liquid crystals are the simplest of all the LCs, wherein the molecules possess long-range orientational order but no positional order. The orientational order in nematic is described in terms of the ability of the molecules to be oriented along a particular direction, referred to as the director (**n**), an apolar vector. When the LC molecules are chiral, the precession of the director in space gives a helical arrangement as seen in the cholesteric ($N^*$); here, the director is perpendicular to the helical axis ($\theta_0 = \Pi/2$). A smectic phase is characterized by a layered structure in addition to the orientational order of the nematic phase [6]. Depending on the molecular arrangements within the layer and the extent of inter-layer correlations, smectic mesophases are classified into different types: Smectic A (SmA), smectic C (SmC) and chiral smectic (SmC*), among others. The relatively young class of bent-core or banana-shaped molecules, owing to their special shape, favour packing into lamellar structures (labelled B1-B8) with a tendency to exhibit the attractive in-plane polar order, anti/ ferroelectric features, and spontaneous chirality despite the molecules being achiral [7,8]. Recently, a new type of nematic phase has been observed known as twist bend nematic ($N_{TB}$) phase, in which the director forms an angle $0 < \theta_0 < \Pi/2$ with the helical axis with the pitch being in the nanometer range [9]. It was found that the $N_{TB}$ phase could be formed by achiral bent molecules, which is locally polar and simultaneously twisted, having a tilted director, the conditions being met by certain flexible dimers with odd linked spacers [10]. Here we are discussing the $N_{TB}$ phase that has been seen in a dimeric material wherein an odd number of atoms in the spacer unit linking the two mesogenic arms [11] gives the molecules their bent shape. Only materials with methylene group as the central spacer exhibit the uniaxial nematic (N) as well as the $N_{TB}$ phase, whereas their ether linkage counterparts, show only the N phase. Notably, in a particular homologous series, that is CBnCB, where n indicates an odd number of methylene units, the existence of $N_{TB}$ and a transition at a higher temperature to its nematic phase has been well established [12].

Apart from the well-known display devices, there are many applications, such as waveguide, beam steering devices etc., in which LC materials are getting increasingly employed as a principal medium. The ensuant electro-optic behaviour forms the basis of these devices. Due to the inherent nature of the LC materials, the devices are passive in that they manipulate the light falling on them but are themselves non-emissive. This built-in lacuna demands a backlight in all but simple alphanumeric devices. In former times, compact fluorescent tubes have been the standard backlight sources, but recently light-emitting diodes and quantum dots are replacing those sources. However, it would be quite attractive if the liquid crystal were itself an emitter. Here we have explored various aspects to get photoluminescence (PL) from liquid crystals by incorporating quantum dots (QDs) and to utilize different techniques to modulate PL. Investigation on nano-soft composites, comprising nanostructures as a guest and liquid crystals as the host material, is one of the emerging research areas for potential applications such as electro-optic devices and displays. The thesis contains seven chapters and one appendix, with Chapter 1 providing the required introduction to the liquid crystal phases. Chapter 2 describes an LC-QD composite, comprising QDs from a special class of materials known as inorganic halide pervoskites (IHPs), which have much higher PL efficiency compared to other II-VI or IV-VI semiconducting QDs. Unlike the latter variety forming spheres, the IHP ($CsPbBr_3$) QDs form quantum cuboids (QCs), and as demonstrated in this Chapter, lead to anisotropic shape entities (2D/3D superstructures) when present in an anisotropic LC medium. More importantly, a novel feature found by us is the appearance of dual anisotropy in emission presumably dictated by the anisotropy of the LC and the capability of the cuboids to form linear chains. These features are further augmented by a fast-switching modulation of PL driven by an applied ac electric field. Chapter 3 illustrates that the photoluminescence from nanocomposites comprising gradient CdSeS quantum dots (QD) doped in a host nematic liquid crystal (LC) can be substantially modulated due to photoisomerization (PI) of small amounts of an incorporated azobenzene-based LC material. Although we could get high photo-driven photo modulation in this work, but the anisotropic PL observed in CsPbBr3 QC/LC composites (Chapter 2) was not observed. We attribute this to the lack of ability of the spherical CdSeS QDs, unlike their perovskite counterparts, to form anisotropic assemblies. As a solution to overcome this problem, in Chapter 4, we demonstrate that dispersing a small amount of CdSeS gradient QDs in an NLC and imposing geometrical confinement of the nanocomposite in a polymer network leads to the regaining of their ordered linear assembly. Such an orientational order is seen not only to enhance the base

photoluminescence but also bring in significant anisotropy in the emission magnitude, a feature barely seen for the system without the polymer network. A further dimension to the studies is added in terms of an improved actinic-light driven PL modulation utilizing a photoisomerizable azobenzene derivative and carefully choosing the QD excitation wavelength. Chapter 5 describes the influence of photoisomerization on a guest-host composite comprising a soft-bent dimer exhibiting the presently sought-after twist-bend nematic ($N_{TB}$) phase, doped with small amounts of a calamitic photoactive azobenzene-based dimer that assumes a bent shape when photo-driven. Chapter 6 demonstrates an easily adaptable procedure to fabricate a switchable smart window of a polymer-stabilized liquid crystalline system (PSLC) formed by a nematic contained in a biopolymer network of cellulose nanocrystals, exhibiting many attractive features. Chapter 7 presents the results on the regular nematic phase of a binary mixture comprising a soft-bent dimer, known in the literature as CB7CB, by incorporating zinc oxide nanorods (ZnO NRs) into the system. There is an increase in anisotropy of the LC system due to the inclusion of the ZnO NRs. Chapter 8 provides an overview of the results presented and an outlook for future developments. A chapter-wise summary of the prominent aspects dealt within the thesis is given below. The last part of the thesis contains an appendix describing a NIR driven photomechanical actuation incorporating porous carbon nanoparticles (PCNs) into polydimethylsiloxane films (PDMS).

## Chapter 1: Introduction to liquid crystals

This Chapter provides a brief introduction to the structure and classification of liquid crystals with emphasis on thermotropic liquid crystals and mention of the relevant basic properties of the nematic phase.

## Chapter 2: Dual anisotropic and fast electrically switchable emission from composites of perovskite quantum cuboids in a nematic liquid crystal

This Chapter describes fast electrically switchable anisotropic photoluminescence from a nano-soft composite comprising a nematic liquid crystal (NLC) and quantum cuboids formed by cesium lead halide ($CsPbBr_3$) perovskite. Quantum dots (QDs) have important implications in a wide range of fields, from photovoltaic to displays to quantum information processing [14,15]. Specifically, the organic/inorganic hybrid perovskites [16], such as $MAPbX_3$ ($MA = CH_3NH_3$; X = Cl, Br, I) QDs, have several attractive features such as high PL and quantum yield, high diffusion length, low processing temperatures, low cost and scalable fabrication. They are potential candidates for use in white LEDs, as wide-colour-

gamut backlight for liquid crystal displays (LCDs), information storage, etc. [15,16] Quantum dots of fully inorganic halide perovskite (IHP) materials such as $CsPbX_3$(X = Cl, Br, I) are becoming popular due to their relatively better stability, significant photovoltaic performances and high PL efficiency (~ 90 %) with concomitant narrow emission line width [13]. Nano-soft composites comprising liquid crystals as host and nanostructures as the guest is an emerging area of research that gets benefitted by the unique characters of the latter in the self-assembling features of liquid crystals [18,19]. The presence of QDs in LC medium improves various electro-optic properties of the host medium [20-24]. It may be highlighted that in the previous cases of LC-QD composites, the QDs are spherical, while in contrast, IHPs form cuboids. Thus, their incorporation into the LC medium can be expected to generate a tendency for self-assembled shape anisotropic structures of QDs. Growth processes which lead to such directionally fixed "QD assemblies" are certainly attractive, and in this regard, the faceted form of the cuboids may facilitate the anisotropic organization.

Despite attempts [20-24] to investigate quantum dot-liquid crystal composites towards switchable emission, perovskite halide systems have not been deployed, owing to their recent appearance on the scene. Being defect tolerant, sharp emission line and high fluorescence levels, these halide systems should prove to be far better candidates than the II-VI semiconductor QDs, and thus the investigations described here establish a new dimension for the field.

Our studies show that the magnitude of the anisotropy in emission (green, $\lambda$ = 514 nm) appears to be dictated by the anisotropy of the LC and the capability of the cuboids to exhibit the novel feature of the formation of a linear chain, the latter being evidenced through optical and electron microscopy, as shown in Figure 1. An applied AC electric field of small amplitude and its consequent coupling to the LC director has been employed to continuously vary the magnitude of the green emission, as depicted in Figure 2. The PL could be dynamically switched by turning the applied electric field on and off. The PL modulation can be obtained in the standard model of addressing (SFP), where the field of time is nearly 40 ms. By appealing to a two-frequency protocol, the emission could be alternated between the anisotropic limits 40 times faster than with a standard protocol. In the main results given in this Chapter, we describe further features of this nanocomposite wherein the system exhibits dual absorption and emission anisotropies – out-of-plane as well as within the plane of the equilibrium orientation of the LC molecules – thus

establishing the wide variety of PL behavior of the investigated nanocomposites.

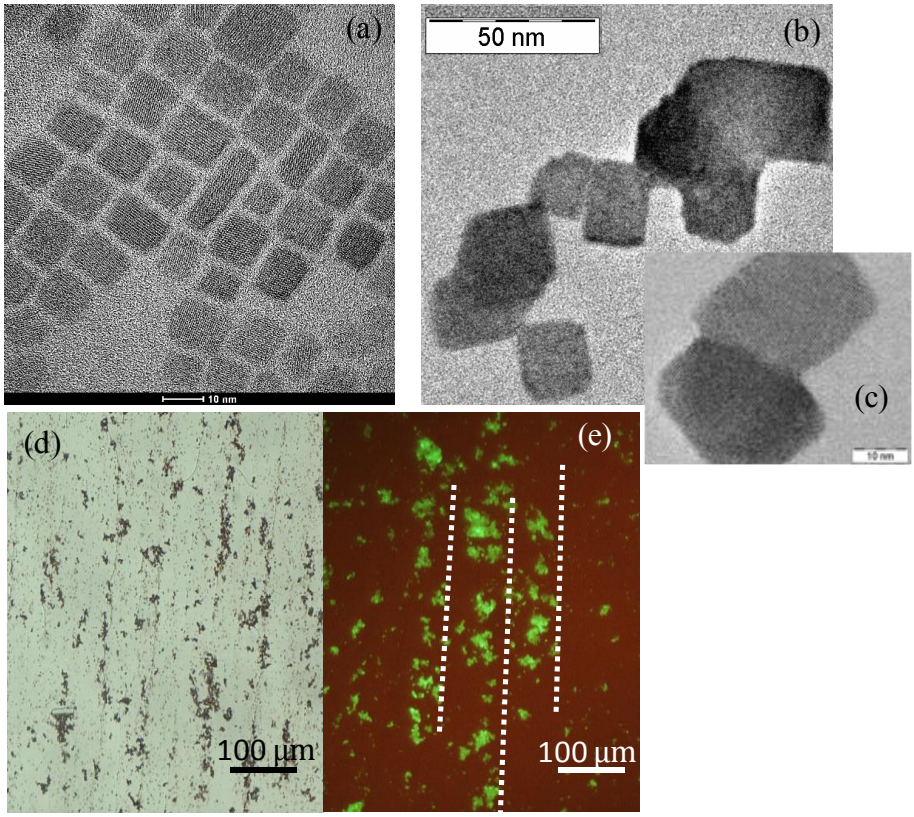


**Figure 1:** *TEM images of (a) the parent CsPbBr3 quantum cuboids (QCs) with an average edge length of 13.7 ±3.1 nm and (b) the same cuboids in the cuboid- liquid crystal (CsLC) composite. The average size of the cuboids remains almost same, whereas the cuboids are seen to have organized in a directed fashion, to result in a linear assembly in the LC medium and (c) When dispersed in the nematic LC, the neighbouring cuboids organize along their body diagonal and develop a tendency to form linear assemblies along the director direction. Polarizing optical microscopy (POM) images in the nematic phase of CsLC at 30 °C captured with (d) white light and (e) excitation light obtained from a 404 nm laser. The linear assembly of QCs along the director direction n is seen as dark objects on the grey nematic background for white light and bright green emission from QC assemblies for 404 nm excitation. The influence of LC birefringence was avoided by removing the analyzer.*

The out-of-plane anisotropy (the X-Z anisotropy), relies on the presence of LC-driven liner assemblies of these QCs and the switching property of the LC molecules to get oriented from surface-dictated planar to field-dictated homeotropic orientation. Application of electric field reorients some of the QCs (QC assemblies) along with the LC molecules to be along Z (out-of-plane direction). This is possible because of the sympathetic communication between the LC molecules and the QCs. By extending these observations, we expect that there is indeed anisotropy present in the (XY) plane containing the LC molecules in the equilibrium (no-field) state.

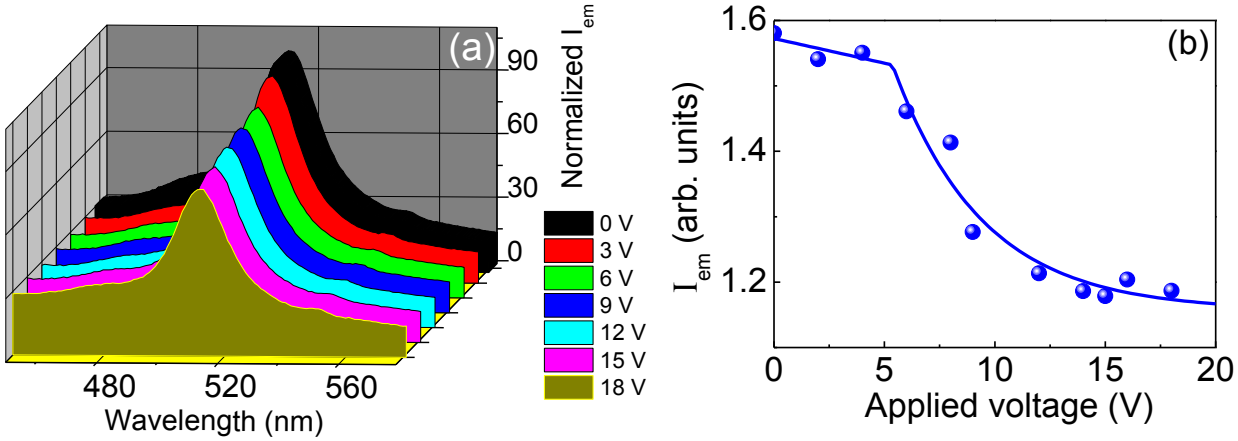


**Figure 2:** *(a) Photoluminescence spectra obtained at room temperature with different applied voltages in the range 0 to 18 V, with the 0 V profile representing the equilibrium planar orientation of the LC molecules with the director parallel to X direction, and the higher voltage profiles approaching the asymptotic situation of homeotropic orientation where the director is parallel to the Z direction. (b) Voltage dependence of the peak emission magnitude exhibiting a clear threshold ~ 6 V and a limiting behaviour at the highest voltage.*

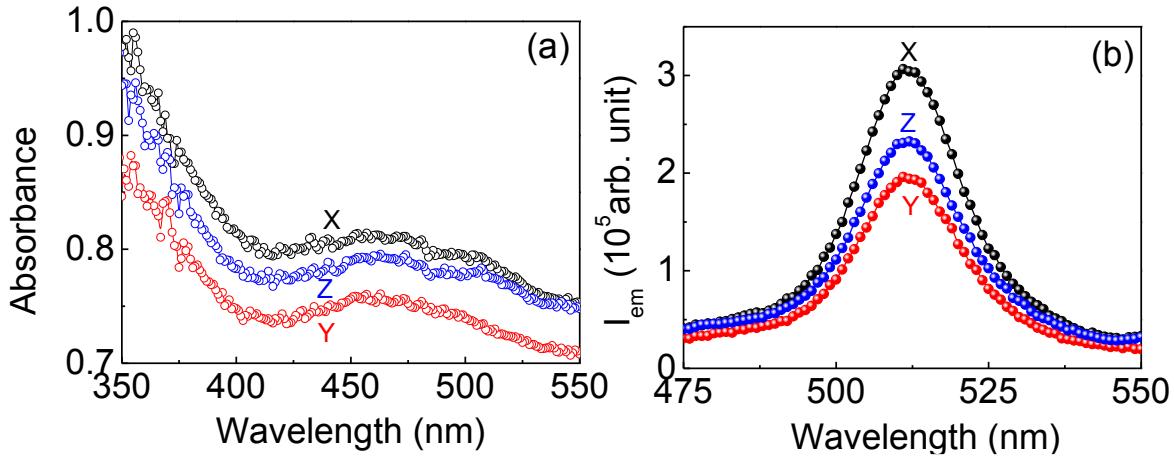


**Figure 3:** *(a) Spectra of $A_X$, $A_Y$ and $A_Z$, the absorbances for the three directions, X, Y and Z. To be noted is that the difference is substantial between $A_X$ and $A_Y$, and less so between $A_X$ and $A_Z$. (b) Photoluminescence spectra at room temperature obtained with excitation at 404 nm for a thin film of the CsLC nanocomposite in the X, Y and Z geometries*

Initially, the data were collected from the X-Y plane, where the cell was kept in such a way that the LC director direction (X) was parallel to the incoming beam polarization axis. Data from the second in-plane direction (Y) was obtained by rotating the cell about the incoming beam axis such that the LC orientation direction (X) is normal to the polarizer direction that was kept fixed. This X-Y difference is significant in comparison with that obtained between the X and Z directions; the latter was achieved by electrical switching of the LC molecules (Figure 3(a)). Figure 3(b) shows the PL spectra obtained with 404 nm excitation of the CsLC nanocomposite in the X, Y and Z configurations.

## Chapter 3: Photoisomerization-driven photoluminescence modulation in CdSeS gradient control quantum dot/liquid crystal nanocomposites

Device control using photo-stimulation has always remained attractive. The photo-control techniques have effectively realized and become versatile because of nanoscience, which has provided multiple pathways to achieve the results. Light as a stimulus has further advantages of having spatial addressing, wavelength and intensity as tunable parameters.

Photo-stimulated isothermal phase transitions in liquid crystal (LC) systems can be brought about by irradiating actinic UV light, which has the capability to alter/stabilize a particular thermodynamic phase [25]. Photoisomerization (PI)– reversible transformation between conformational isomers –of azobenzene derivatives is one of the popular photo-stimulated processes. Despite the fact that the effect can be large if the entire material is photoactive, having small quantities of a guest photoactive material in a host non-isomerizing LC system is found to be more attractive from an experimental point of view[25]. Here we have employed gradient controlled CdSeS QDs. These QDs show a high PLQY, which can go up to as high as 85%.

The main focus of the Chapter is to get PI-driven photoluminescence (PL) modulation in LC+QD nanocomposites. The transition between the nematic and the isotropic phases driven by temperature can be achieved under isothermal conditions by employing the process of photoisomerization. The shape change of the minority azobenzene derivative (EPH for short) employed can effectively bring this about while changing their isomeric conformation from *trans* to cis under the influence of actinic light (UV: 365 nm).The photoisomerization of the EPH molecules drastically reduces (by 45%) the PL intensity (Figure 4(a)).

The attractive aspect is that upon turning off the actinic (UV) light, the system essentially recovers the original profile as seen in Figure 4(a). A PL switch operating between the high PL “equilibrium” nematic and the low PL “photo-driven” isotropic phases under isothermal conditions is shown in Figure 4(b). It is quite striking that the PL swing is quite large (~ 30%). The PI-driven state gets achieved very quickly, but the recovery of the equilibrium value upon turning the UV off, being controlled by the thermal back relaxation(TBR) mechanism, is slow as indeed expected. However, we show that the slow PL recovery can also be accelerated by an applied field having a suitable frequency protocol.

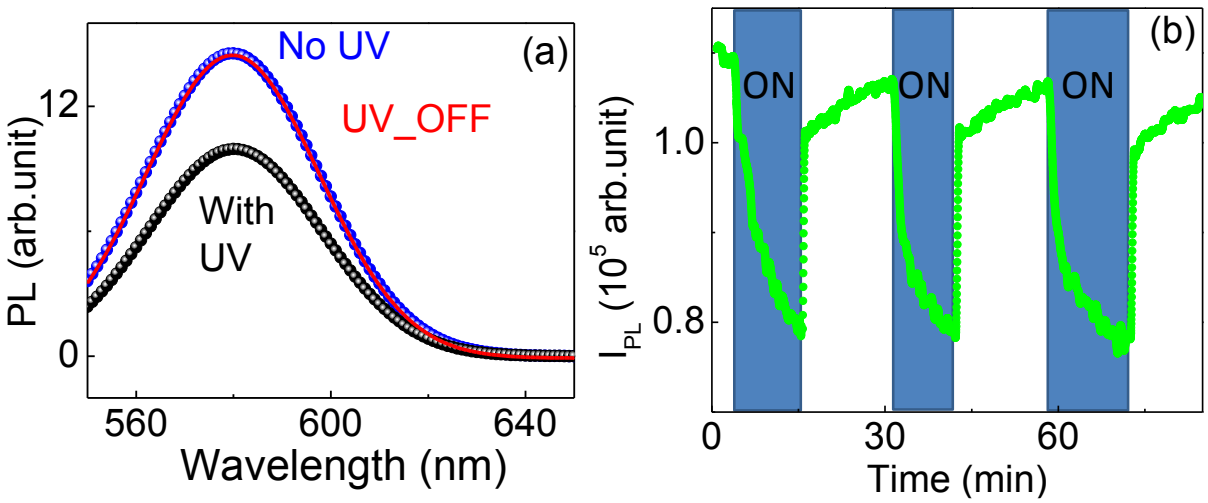


**Figure 4:** *(a) The emission spectra for one of the nanocomposites under No UV (blue symbols) and with UV (black symbols) conditions, depicting a 45% reduction in the emission between the two situations and the recovery of the PL values after the UV off (red line).(b) Dynamics of PL process arising from QD emission driven by photoisomerization of EPH molecules. Upon turning the UV on, PL drops precipitously and quickly achieves a limiting value. The PL modulation controlled by the photoisomerization process is well reproduced over several cycles.*

## Chapter 4: Enhanced luminescence, electric-field and actinic-light modulation of emission in nematic-CdSeS gradient nanocrystal composites by polymer confinement

In this Chapter, we have further implemented complementary aspects to the photo-driven PL described in the previous Chapter. Here, by incorporating the material in a polymer network we could enhance both the absolute value of the photoluminescence arising from the QDs as well as the electrically modulated anisotropic emission. The presence of the network substantially improves the photo modulated PL dynamics. Large anisotropic ratios are achieved, despite the fact that the employed QDs are spherical CdSeS gradient nanostructures. The pathways appeal to (i) having a second LC component which is dichroic and (ii) creation of virtual surfaces by confining the LC+QD composite in an *in situ* created polymer network. Through electron microscopy imaging, the polymer network is seen to impart a self-assembled orientational order to the ensemble of QDs, as seen from Figure 5. The base system, referred to as E7Q, consisting the nematic eutectic mixture E7 and QDs, was used to prepare further composites, E7Po (E7Q+5% PMMA), E7Ph (E7Q+4.5 mol% of EPH) and E7PoPh (E7Q+5% PMMA+4.5 mol% of EPH). Here PMMA refers to the polymer, polymethyl methacrylate.

The main interest was to exploit the inherent orientation-dependent anisotropic characteristics of the LC and the possibility to extract anisotropic PL from the QDs owing to their self-assembly by the LC host. It should be emphasized that the self-assembly was dictated by the oriented polymer network. Figure 6 depicts the dynamic PL switching of the different LC nanocomposite mixtures when an electric field of 20 V, 1 kHz sine wave is switched on and subsequently off. For all mixtures studied, the field-driven quenching and restoration of PL upon turning the field off are quite sharp, happening within a few seconds. As indeed expected from the discussions made above, the E7Q materials have the least PL modulation and E7PhPo, the highest.

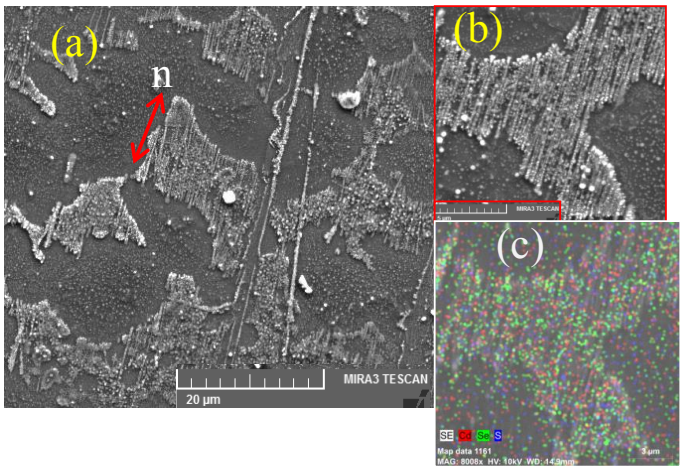


**Figure 5:** *(a) and (b)Scanning electron microscopy images of the QD+LC polymer nanocomposite. The nematic director direction fixed by the aligning polymer layer (denoted by red arrow in panel (a)) governs the orientation direction of the polymer that forms the network confining the LC. Interestingly, it plays the role of self-assembling the QDs (bright dots) in linear arrays, which in turn, is responsible for the anisotropy in emission. This is amply demonstrated by the energy-dispersive X-ray spectroscopic (EDXS) image (panel (c))of the area shown in (b).*

Figure 7(a) and (b) show the PL recovery, after switching the UV off, due to the thermal back relaxation (TBR), a phenomenon certainly known to be slow. However, it may be noted that the presence of the polymer network does decrease the TBR response time ($\tau_{off}$) by 30%.

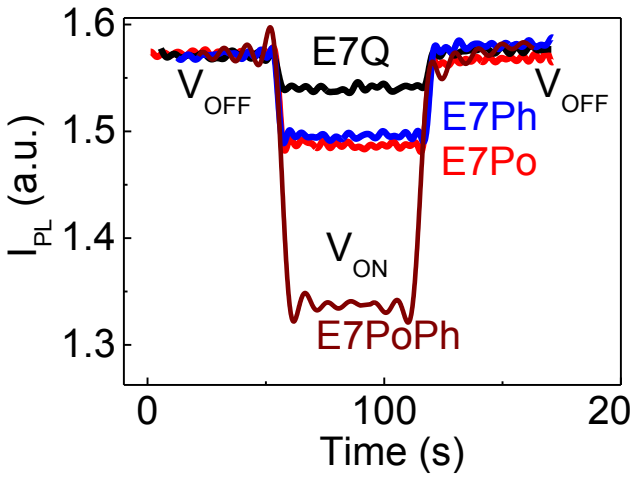


**Figure 6:***Field driven dynamic PL switching profiles for E7Q, E7Ph, E7Po and E7PoPh composites. Turning the field ON ($V_{ON}$), the PL value decreases to a minimum value, and the equilibrium value is restored after switching the field OFF ($V_{OFF}$). The much weaker PL modulation magnitude for E7Q, E7Ph and E7Po samples is significantly enhanced for the E7PoPh sample.*

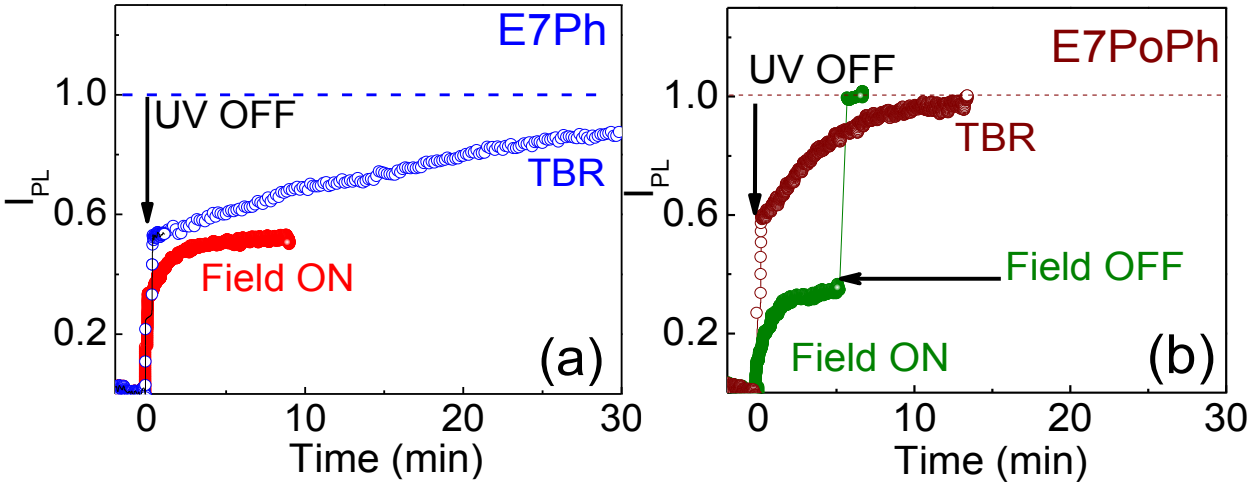


**Figure 7:***The return of equilibrium PL values after switching the UV radiation off. There are two temporal dependences in the PL-return profiles for both samples. In both materials, the slower curves (open symbols) are due to the thermal back relaxation (TBR) of the cis conformers of EPH molecules, although much slower in the non-polymer case. However, the TBR process can be accelerated by applying a DC bias of 40 V (closed circles). A feature that must be borne in mind is that the field ON state also reorients the LC molecules to be along the field direction leading to a much lower saturated value of PL. If indeed, the field is applied only for a short duration and then removed, the original equilibrium PL value can be quickly realized as shown in panel (b).*

## Chapter 5: A soft-bent dimer composite exhibiting the twist-bend nematic phase: photo-driven effects and an optical memory device

The *trans* - cis photoisomerization causes a lowering in the ordering of the LC systems, as described in the previous Chapters. Whereas the consequent effects have been well studied

for rod-like LCs, the rigid bent-core LCs have been investigated only recently [26]. Our motivation was to soften the bent portion of the molecules and study the influence of photoisomerization. For this purpose, we chose a guest–host system wherein both components are dimers. The host is a soft-bent dimer (CB7CB) that shows the $N_{TB}$ phase and a photoactive guest azobenzene–based dimer (4AOA4). It may be mentioned that the host, as well as the guest-host mixture employed, exhibit the nematic - $N_{TB}$ phase sequence. In the following, we describe some of the consequences due to photoisomerization.

The temperature dependence of the splay elastic constant $K_{11}$, without and upon UV illumination of different intensity levels ($I_{UV}$ =3, 5 and 8 mW/cm$^2$), increases with decreasing temperature. This feature is expected due to its association with the orientational order parameter. However, upon photoisomerization, the value substantially diminishes; for example, at $T_N$ –20 K, the reduction is by 25%. The main attraction is that with the increase in $I_{UV}$, the $K_{11}$ values get lowered without affecting the increasing trend observed for $K_{11}$. Such large changes in $K_{11}$ by merely photo-driving the shape (from rod-like to bent-form) of the minority (5% 4AOA4) constituents were achieved.

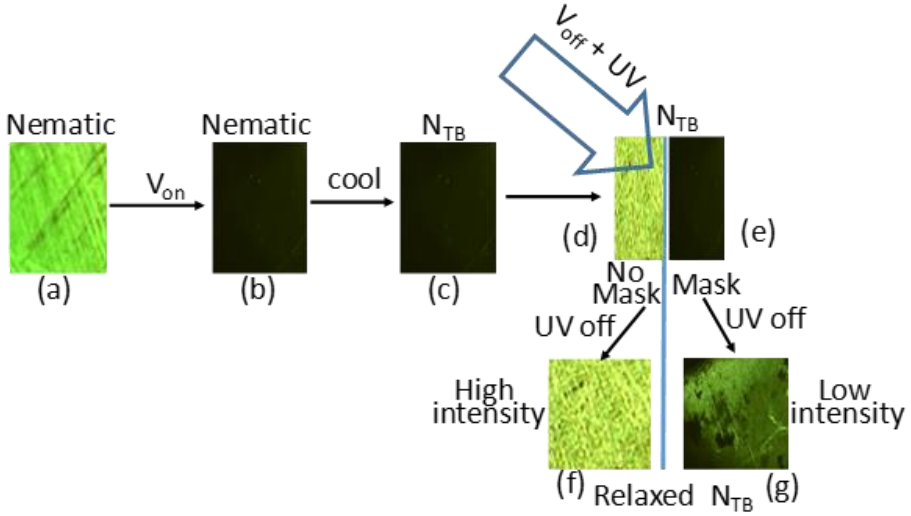


**Figure 8:** *Demonstration of the memory device based on the optical texture retention in the $N_{TB}$ phase. The protocol followed is: An electric field of suitable magnitude applied to a planar nematic turns the field of view from birefringent (a) to a dark one (b). Keeping the field on, if the sample is cooled to $N_{TB}$, the field of view remains dark (c). At this stage, if the sample is illuminated with UV light through a photomask and after a short while the field is turned off, then the region without the mask will transform to the photo-driven N phase and since the field is off takes the birefringent texture (d). The masked region, not having undergone photoisomerization remains in the $N_{TB}$ and thus continues to have a dark field of view (e). Even after a time sufficiently longer than the relaxation time these two regions (f and g respectively) exhibit significant contrast difference, a feature necessary for an optical memory device.*

The dynamics of the photo-driven transitions and the thermal back relaxation have been investigated. Upon UV irradiation on the system, the equilibrium N phase transforms to the isotropic phase. Similarly, if the equilibrium is $N_{TB}$, it transforms to the driven N phase. It is found that, unlike in rod-like systems, the response of the back relaxation process is also fast. The system is fatigue-free as seen from highly responsive changes in the magnitude of switching over a large number of cycles. We have been demonstrated that an optical memory device can be conveniently fabricated using this principle (Figure 8). The device exhibits good optical contrast.

**Chapter 6: Switchable smart windows using a biopolymer network of cellulose nanocrystals imposed on a nematic liquid crystal**

There is an increasing demand for smart, dynamic windows capable of electrically controlling the transmitted light level for aesthetics, privacy control, automotive and improved energy efficiency applications [27-34]. Several competing technologies have come up for such applications [35-39]. Polymer dispersed, and polymer-stabilized liquid crystals (PDLC and PSLC) are two important LC-dependent systems [40]. Between these two, the PSLCs comprising a small quantity of a polymer forming a network are further attractive owing to lower driving voltage compared to their PDLC counterparts. But they also do have drawbacks. In this Chapter, we have investigated a biopolymer network formed by cellulose nanocrystals (CNC) to confine a nematic LC for creating smart windows that overcome these drawbacks; the CNCs were extracted from discarded groundnut shells. The fabrication process is much simpler than a recently reported one that has a more involved preparation protocol [40].

All the nanocomposites investigated here, spanning the concentration range of X = 0 to 10 (X is the weight % of CNC in the CNC/LC mixture), were confirmed by polarizing optical microscopy (POM) observations to exhibit the nematic mesophase at room temperature, a prerequisite for these studies.

The POM image in the nematic phase clearly shows (Figure 9(a)) the existence of the CNC network having large voids, which are, in fact, regions where the LC material is present. To be noted is also the absence of any orientational order of the polymer strands defying the expectation for PSLC. The formation of networks of polymer fibres is even more clearly visualized in the FESEM image obtained after leaching out the LC (Figure 9(b)). The network is indeed seen to be random, as opposed to the aligned networks of a standard PSLC.

This loose circular-like void network has similarities with the *Swiss-cheese* architecture, seen earlier in systems wherein the polymer network is mechanically strengthened by reinforcing with CNT or graphene [42,43].

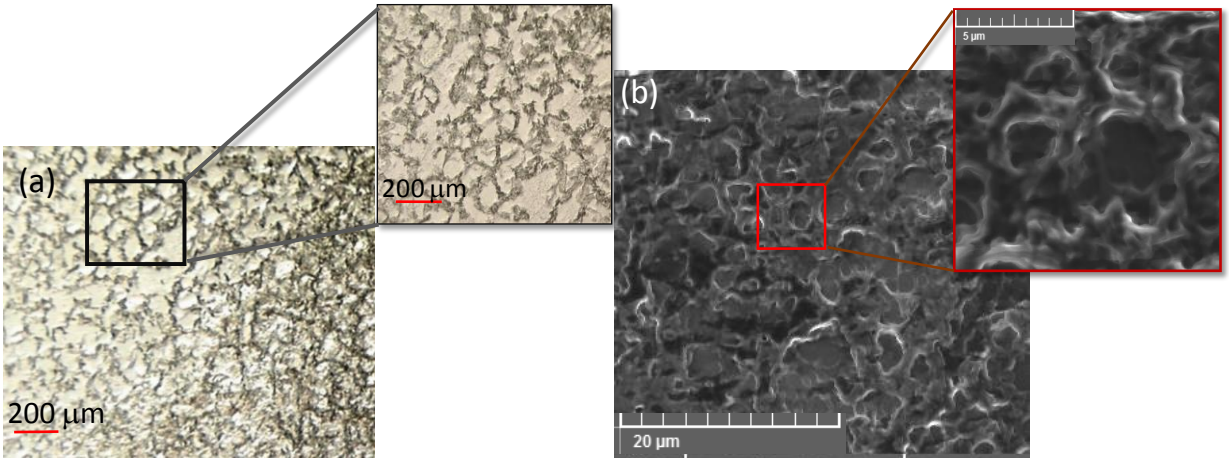


**Figure 9:** *Images exhibiting the network formation at two length scales: (a) polarizing optical microscope image, in which the anlayzer was removed to prevent the domination of the sample birefringence. (b) FESEM image clearly bringing out the Swiss-cheese architecture of the network as opposed to the fibrous morphology. The insets in both cases are the enlarged versions of the indicated squares of the main image.*

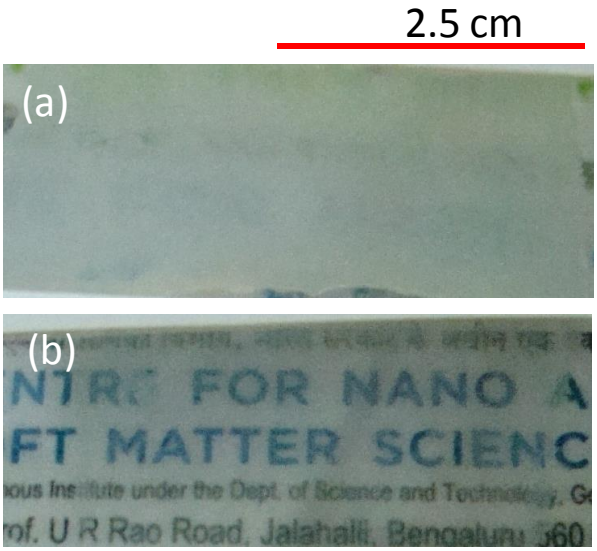


**Figure 10:** *Fabricated smart window device in the (a) scattering and (b) transparent states. The text kept behind the device can be clearly seen in (b), but not in (a).*

The threshold or the minimum voltage needed to operate the electro-optic device does not depend on the concentration of the polymer, a feature in contrast to the standard PSLC systems. A second point, more important from the driving circuit point of view, is that the voltage-off response time drastically reduces and even becomes practically invariant over the thermal range of the nematic phase. Encouraged by the observation of a scattering state in the equilibrium situation, and it turning into a transparent state when the electric field is applied,

we fabricated a smart window using the 7CB/CNC system; 7CB is the well-known heptyl cyano biphenyl. The images of the fabricated CNC based PSLC smart window device are presented in Figure 10. A printed text kept behind and viewed through the device is hardly seen in the field-off scattering state (Figure 10(a)) but quite clear in the field-driven transparent state (Figure 10(b)), resulting in good contrast.

## Chapter 7: Influence of Zinc Oxide nanorods an orientationally ordered fluid comprising soft-bent dimmers

One of the most fundamental properties of an LC, that gets influenced by shape changes of the constituent entities is the transition temperature, especially the clearing point, i.e., the nematic-isotropic (N-I) transition (TNI). While these studies have been well explored in terms of the shape of the molecule responsible for liquid crystallinity, incorporating nanostructures into LC for this purpose is a recent trend. The large body of work already created in this direction involves spherical particles, always resulting in lowering TNI with respect to the value for the pristine LC [44]. Even with anisotropic nanostructures, the changes seen are marginal. The prime reasons for this are (a) the shape anisotropy (aspect ratio) of the nanostructures incorporated has been either too small or too large and (b) the host LC and the nanostructure have essentially the same shape. Keeping these features in mind, we have chosen as the host LC a binary system consisting of a short rod-like molecule (heptyloxy cyanobiphenyl) and a soft-bent dimer (CB7CB) [45]. Ignoring any size difference between the two LC molecules, the shape anisotropy of the host can be taken to be ~6. As dopant nanostructures, we chose ZnO nanorods, which have only a slightly higher aspect ratio, and of course, are stiff rods. For this purpose, vertically grown ZnO nanorods (NRs) were synthesized by a hydrothermal process. Figure 11 shows the FESEM images of the grown nanorods. The size histograms indicate the length to be 259±4 nm and diameter to be 1.86±0.048 μm, giving an aspect ratio of 7.2±0.05. The composites are indicated as HLCmZ, where m is the concentration of ZnO NRs in the mixture.

For the LC-NR composites, a substantial increase in TNI is indeed observed, demonstrating the importance of the tuning of the shape anisotropy of the two kinds of entities to achieve the objective at hand. This is supported by differential scanning calorimetry (DSC) studies obtained for HLC and the two composites. Figure 12 shows permittivity measurements in two geometries, with the director being parallel ($\varepsilon_{\parallel}$) and perpendicular ($\varepsilon_{\perp}$) to the probing field. The shifts in $T_{NI}$ observed here match with those from DSC scans. For HLC1Z, $\varepsilon_{\parallel}$ is hardly changed but $\varepsilon_{\perp}$ is lowered by 4%. In contrast, HLC4Z shows larger reductions in both $\varepsilon_{\parallel}$ (9%) and $\varepsilon_{\perp}$ (5.5%).

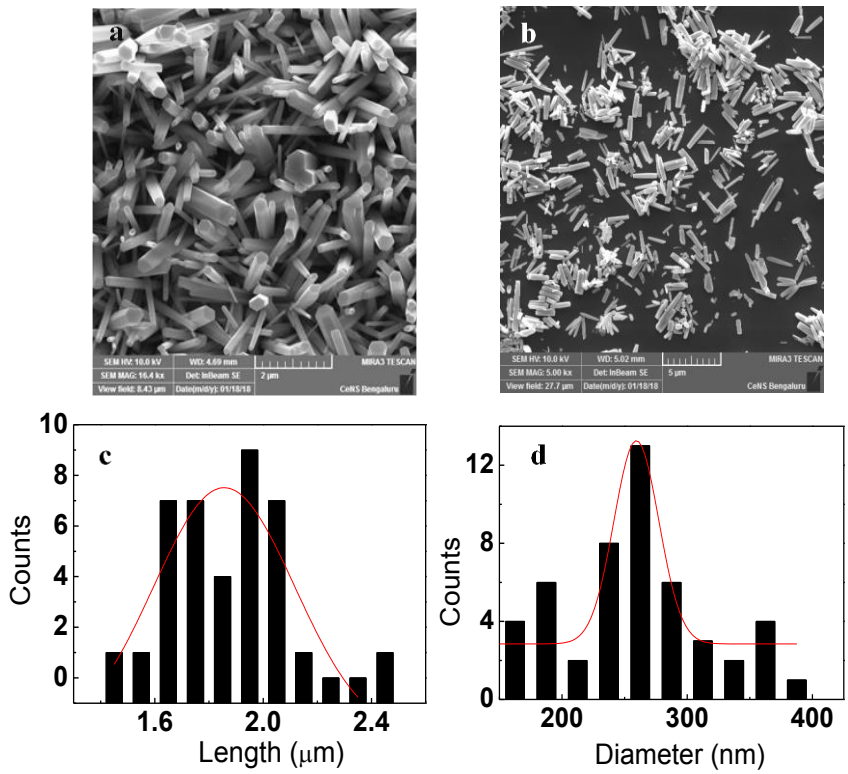


**Figure 11:** *FESEM images of ZnO NRs grown on (a) a glass plate and (b) drop cast after dispersion in methanol, exhibit a very well defined rod shape with a hexagonal cross-section. Panels (c) and (d) show the size histograms.*

These observations clearly point to an increase in the orientational order parameter of the system due to the addition of NRs, a result that has been confirmed with an increase in birefringence for the composites. Further support is seen in terms of lowered $\Delta\varepsilon$ indicating a better dipolar coupling between the polar host molecules, causing improved cancellation of dipole moment in the director direction. These features bring out the importance of the shape and aspect ratio of the dopant nanostructures.

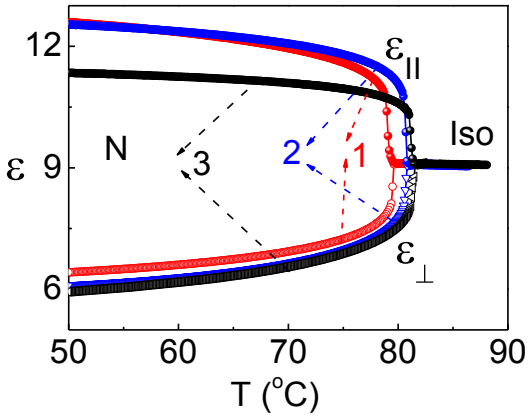


**Figure 12:** *Thermal variation of permittivity parallel ($\varepsilon_{||}$) and perpendicular ($\varepsilon_{\perp}$) to the nematic director [made to have a matching isotropic value ($\varepsilon_{iso}$)] for the HLC material (dataset 1) and for the nanocomposites, HLC1Z (dataset 2) & HLC4Z (dataset 3).*

## Chapter 8: Outlook

This section provides a comprehensive overview of the work described in the other chapters along with their potential applications and a future outlook.

## Appendix

### Large magnitude fast photomechanical actuation in PDMS – porous nanocarbon composites

Here we demonstrate that imbibing porous carbon nanoparticles (PCNs) in polydimethylsiloxane (PDMS) single-layer films yields NIR-driven photomechanical actuation. A further advantage of the presently used PCNs is that they are obtained from a bio-waste source. Photomechanical actuation depends on various physical characteristics of the PCNs, one of the primary ones being the surface area of the pores. This parameter controlled using the pyrolization temperature and varied over a factor of 600, is seen to have a strong influence on the magnitude of the actuation as well as the time response of actuation and relaxation processes. The curing agent used for polymerizing PDMS is found to be another parameter of importance. Further, the actuation gets enhanced by as much as a factor of two due to the presence of an ultrathin gold backing layer. The observed feature that the direction of photo-driven deflection is opposite for the single and bilayer films itself is an attractive feature and adds to possible applications. Employing the bilayer films, a simple photo-stimulated LED switch is also presented. The results bring out the potential of these films for bioengineering applications, and lay the basis to bring in anisotropic LC systems to act as the anisotropic materials to tune/modulate the actuation.

## References


[1] S. Chandrasekhar, Liquid Crystals, Cambridge University Press New York, 2nd Ed. (1992).

[2] I. Hamley, Introduction to Soft Matter (2nd edition), J. Wiley, Chichester (2000).

[3] P. G. de Gennes and J. Prost, The Physics of Liquid Crystals, Oxford Science Publication, Oxford, (1993)

[4] P. J. Collings and M. Hird, Introduction to Liquid Crystals:Chemistry and Physics, Taylor and Francis Ltd. London, (1997).

[5] D. K. Yang and S.T. Wu, Fundamentals of Liquid Crystal Devices, John Wiley Sons, Ltd., ( 2006).

[6] K. K. Kobayashi, *Phys. Lett.*, **31A**, 125 (1970).

[7] T. Niori, T. Sekine, J. watanabe, T. Furukawa and H. Takezoe, *J. mater. Chem*., **6**, 1231 (1996).

[8] D.R. Link, G. Natale, R. Shao, J.E. Maclennan, N. A. Clark, E. Korblova and D.M. Walba, *Science*, 278, 1924 (1997).

[9] PanovV P, Nagaraj M, VijJ K, Panarin Y P, Kohlmeier A, Tamba M G, Lewis R A and Mehl G H*Phys. Rev. Lett.* **105**,167801 (2010).

[10] Cestari M, Frezza E, Ferrarini A andLuckhurst G R*J. Mater. Chem.***21,** 12303 (2011); Chen D,Porada J H,Hooper J B,Klittnick A, Shen Y M,TuchbandM,KorblovaE,BedrovD,Walba D M,Glaser M A,Maclennan J Eand Clark N A *Proc. Natl.Acad. Sci.***110**,15931 (2013).

[11] D. A. Paterson, M. Gao, Y.K. Kim, A. Jamali, K. L. Finley, B.R. Hernandez, S. D.Berart, J. Salud, M. Rosario de la Fuente, B. A. Timimi, H. Zimmermann, C. Greco, A. Ferrarini, J.M. D. Storey, D. O. Lopez, O.D. Lavrentovich, G. R. Luckhurst and C. T. Imrie, *Soft Matter*, **12**, 6827 (2016).

[12] M. Cestari, S. Diez-Berart, D. A. Dunmur, A. Ferrarini, M. R. de la Fuente, D. J. B. Jackson, D. O. Lopez, G. R. Luckhurst, M. A. Perez-Jubindo, R. M. Richardson, J. Salud, B. A. Timimi and H. Zimmermann, *Phys. Rev. E*, **84**, 031704 (2011).

[13] R. S. Liu, Phosphors, Up Conversion Nano Particles, Quantum Dots and Their Applications, Springer 2016.

[14] J. J. Choi, W. N. Wenger, R. S. Hoffman, Y. F. Lim, J. Luria, J. Jasieniak, J. A. Marohn, T.Hanrath, Adv. Mater. **23**, 3144 (2011).

[15] C. H. Chuang, P. R. Brown, V. Bulovic, M. G. Bawendi, Nat. Mater. 2014, **13**, 796.

[16] R. Sheng, X. Wen, S. Huang, X. Hao, S. Chen, Y. Jiang, X. Deng, M. A. Green , A. W. Y. Ho-Baillie, Nanoscale **8**, 1926 (2016).

[17] Y. H. Kim, H. Cho, J. H. Heo, T. S. Kim, N. Myoung, C. L. Lee, S. H. Im, T. W. Lee, Adv. Mater. **27**, 1248 (2015).

[18] X. Dai, Y. Deng, X. Peng, Y. Jin, Adv. Mater. **29**, 1607022 (2017).

[19] H.-W. Chen, R.-D. Zhu, J. He, W. Duan, W. Hu, Y.-Q. Lu, M.-C. Li, S.-L. Lee, Y.-J. Dong, S.-T. Wu, Light Sci. Appl. **6**, e17043 (2017).

[20] I. Dierking, G. Scalia, P. Morales, D. LeClere, Adv. Mater. **16**, 865 (2004).

[21] S. Krishna Prasad, M. Baral, A. Murali, S. N. Jaisankar, ACS Appl. Mater. Interfaces **9**, 26622 (2017).

[22] P. L. Madhuri, S. K. Prasad, S. Pravin, B. L. V. Prasad, Appl. Phys. **49**, 425304 (2016).

[23] B. Kamaliya, M. Vijay Kumar, C. V. Yelamaggad, S. Krishna Prasad, Appl. Phys. Lett. **106**, 083110 (2015).

[24] D. Wang, D. Wu, D. Dong, W. Chen, J. Hao, J. Qin, B. Xu, K. Wang, X. Sun, Nanoscale **8**, 11565(2016).

[25] T. Kosa, L. Sukhomlinova, L. Su, B. Taheri, T.J. White, and T.J. Bunning, Nature **485**, 347 (2012)

[26] P. Lakshmi Madhuri, S. Krishna Prasad, Uma S. Hiremath, and C. V. Yelamaggad Appl. Phys. Lett., **104**, 241111 (2014)

[27] F. Gonzalez, Smart Windows and Smart Glass 2014-2024: Technologies, Markets, Forecasts, (IDTechEx) (n.d.).

[28] J. Kim and J.I. Han, Electron. Mater. Lett. 10, 607 (2014).

[29] A. Hinojosa and S.C. Sharma, Appl. Phys. Lett. 97, 81114 (2010).

[30] A. Masutani, T. Roberts, B. Schüller, N. Hollfelder, P. Kilickiran, A. Sakaigawa, G. Nelles, and A. Yasuda, J. Soc. Inf. Disp. 16, 137 (2008).

[31] E. Kim, Y. Liu, S.-J. Hong, and J.I. Han, Nano Converg. 2, 5 (2015).

[32] H. Hakemi, M. Caporusso, and M. Santangelo, US6049366 A (2000).

[33] C. Su, K. Yang, and J. Lien, US 20140016078 A1 (2014).

[34] R.R. Deshmukh, Liquid Crystalline Polymers, Vol.2-Proc (Springer International Publishing, Switzerland, n.d.).

[35] T. Xu, E.C. Walter, A. Agrawal, C. Bohn, J. Velmurugan, W. Zhu, H.J. Lezec, and A.A. Talin, Nat. Commun. 7, 10479 (2016).

[36] L. Wang, Y. Liu, X. Zhan, D. Luo, and X. Sun, J. Mater. Chem. C 7, 8649 (2019).

[37] S.N. Alamri, Sol. Energy Mater. Sol. Cells 93, 1657 (2009).

[38] H. Ren, S. Xu, and S.-T. Wu, Opt. Lett. 37, 1421 (2012).

[39] B. Lamontagne, N.R. Fong, I.-H. Song, P. Ma, P.J. Barrios, and D. Poitras, J. Micro/Nanolithography, MEMS, MOEMS 18, 1 (2019).

[40] I. Dierking, Polymer-Modified Liquid Crystals (The Royal Society of Chemistry, 2019).

[41] Q. Liu and I.I. Smalyukh, Sci. Adv. 3, e1700981 (2017).

[42] S. Krishna Prasad, M. Baral, A. Murali, and S.N. Jaisankar, ACS Appl. Mater. Interfaces 9, 26622 (2017).

[43] M. Baral, K. Bramhaiah, N.S. John, and S. Krishna Prasad, ACS Omega 4, 403 (2019).

[44] Basu R, Sigdel K P and Iannacchione G S Eur. Phys. J. E **34**, 34 (2011).

[45] S. Parthasarathi, D.S.S. Rao, N.B. Palakurthy, C.V. Yelamaggad and S.K. Prasad, *J. Phys. Chem. B***120**, 5056 (2016).

## The following is the list of publications resulting from the work carried out by the candidate and in the order appearing in the text:

1. **Pragnya Satapathy**, V. Navyashree, James Oinam, S. K. Prasad, 'Enhanced luminescence and electric-field modulation in nematic-CdSeS gradient nanocrystal composites by polymer confinement.' *J. mol. Liq.* (2021), *https://doi.org/10.1016/j.molliq.2021.118004*
2. **Pragnya Satapathy**, Raghavendra Adiga, Monish Kumar, Gurumurthy Hegde and S. Krishna Prasad, 'Large magnitude fast photomechanical actuation in PDMS – porous nanocarbon composites.' *J. Nanostruct. Chem.* (2021), *https://doi.org/10.1007/s40097-021-00414-9*
3. **Pragnya Satapathy**, Srividhya Parthasarathi, DS Shankar Rao, Saleheen Bano, Yuvraj Singh Negi, S Krishna Prasad, 'Switchable smart windows using a biopolymer network of cellulose nanocrystals imposed on a nematic liquid crystal.' *Appl. Phys. Lett.* **117**, 103702 (2020)
4. **Pragnya Satapathy**, V. Navyashree, P. K. Santra, S.K. Prasad, 'Photoisomerization-driven photoluminescence modulation in CdSeS gradient quantum dot/liquid crystal nanocomposite.' *Chem. Photo. Chem.* **4**, 413 (2020)

5. **Pragnya Satapathy**, Pralay K. Santra and S, Krishna Prasad, 'Synergistic path for dual anisotropic and electrically switchable emission from a nanocomposite of CsPbBr3 quantum cuboids and nematic liquid crystal.' *Crystals.* **9**, 378 (2019)
6. **Pragnya Satapathy**, Pralay K Santra, Anamul Haque, C.V. Yelamaggad, Shyamashis Das, S Krishna Prasad, 'Anisotropic Fast Electrically Switchable Emission from Composites of CsPbBr3 Perovskite Quantum Cuboids in a Nematic Liquid Crystal.' *Adv. Opt. Mat.* **7**, 1801408 (2019)
7. **Pragnya Satapathy**, Srividhya Parthasarathi, D.S. Shankar Rao and S. Krishna Prasad, 'Influence of Zinc Oxide nanorods on an orientationally ordered fluid comprising soft-bent dimers.' *Bull. Mater. Sci.* **41**, 116 (2018)
8. S. Krishna Prasad, P. Lakshmi Madhuri, **Pragnya Satapathy** and C.V. Yelamaggad, 'A soft-bent dimer composite exhibiting twist-bend nematic phase: photo-driven effects and an optical memory device.' *Appl. Phys. Lett.***112**, 253701 (2018)

Details of the patent application based on the above research work are included in the thesis:

1. A polymer doped liquid crystal composition and method thereof, Patent date: Filed April 10, 2018, Indian Patent; Application no- 202041000263

A book chapter has a partial contribution from the research work presented in this thesis:

1. 'Liquid crystals in one-dimensional polymeric nano networks: Physics and applications.' Pragnya Satapathy, Divya Jyoti and S. Krishna Prasad, CRC Press/Taylor and Francis Group, 2021 (book chapter submitted)

In addition, the candidate is also an author of collaborative published articles with other research groups

1. Supreet Kaur, Golam Mohiuddin, **Pragnya Satapathy**, Rajib Nandi, Vidhika Punjani, S Krishna Prasad, Santanu Kumar Pal, 'Influence of terminal halogen moieties on the phase structure of short-core achiral hockey-stick-shaped mesogens: design, synthesis and structure–property relationship.' *Mol. Sys. Desig.& Eng.* **3**, 839-852 (2018)
2. K Maji, P Acharry, **Pragnya Satapathy**, S K Prasad, K Biswas, 'Mechanochemical synthesis and temperature dependent optical poroperties of thermochromic $(Ag_{1-x}Cu_x)_2HgI_4$.' *Chem. Asian J.* **14**, 4641 (2019)

## List of conferences and workshops attended

### Conferences

1. "24thNational Conference on Liquid Crystals (NCLC-2017)" 7-9 October 2017, organized by Department of Chemical Sciences, IISER Mohali, Mohali-140306 (poster presentation)

2. "9th Bangalore INDIA Nano" 7-8 Dec 2018, organized by Department of IT, Biotechnology and Science & Technology, Government of Karnataka (*poster presentation*)

3. "International Conference in Nano Science and Technology (ICONSAT 2018)" 21-23 March 2018, organized by Centre for Nano and Soft Matter Sciences, Bengaluru-560013 (*poster presentation*) **(*Best poster award*)**

4. "25th National Conference on Liquid Crystals (NCLC-2017)" 19-21 December 2018, organized by Centre of Materials Science, University of Allahabad, in association with National Academy of Sciences India (NASI) (*oral presentation*)

5. "9th MRS Trilateral Conference on Advances in Materials: Energy, Water and Healthcare " 22-24 October 2018, organized by Centre for Nano and Soft Matter Sciences, Bengaluru-560013 (*poster presentation*) **(*Best poster award*)**

6. "ChemPhysMat 2019 conference" 20-22 Feb, 2019, organized by Jawaharlal Nehru Centre for Advance Scientific Research, Bengaluru (*poster presentation*)

7. "26th National conference on Liquid Crystals (26th NCLC)" 21-23 October, 2019, organized by Chitkara University Research and Innovation Network (CURIN), Department of Applied Sciences, Chitkara, Patiala, Punjab (*poster presentation*) **(*Best poster award*)**

### Workshops

1. 'Soft and Active Matter workshop' 11-17 February 2018, organized by University of Hyderabad, School of Physics UGC-networking resource centre & DST-purse

2. 'Nano Mission School on Nanoscience & Nanotechnology – Physical Sciences(Emerging Materials and Methods in Nanoscience & Nanotechnology)' 23

October 23 to 3 November, 2017, organized by Centre for Nano and Soft Matter Sciences, Bangalore

(PRAGNYA SATAPATHY)

Forwarded through

Dr. S. Krishna Prasad
(Research Supervisor)

Head of the institution